

# Quantum Hall Criticality, Superconductor-Insulator Transition and Quantum Percolation

Yonatan Dubi<sup>1</sup>, Yigal Meir<sup>1,2</sup> and Yshai Avishai<sup>1,2</sup>

<sup>1</sup> *Physics Department, Ben-Gurion University, Beer Sheva 84105, Israel*

<sup>2</sup> *The Ilse Katz Center for Meso- and Nano-scale Science and Technology, Ben-Gurion University, Beer Sheva 84105, Israel*

(Dated: March 14, 2022)

A model consisting of a mixture of superconducting and quantum links is proposed to describe the integer quantum Hall transition. The quantum links correspond to tunneling of electrons between trajectories trapped in adjacent potential valleys, while the superconducting links correspond to merging of these trajectories once the Fermi energy crosses the saddle point energy separating the two valleys. The quantum Hall transition in this model corresponds to percolation of the superconducting links. Numerical calculations and scaling analysis using two different approaches yield the critical exponent  $\nu \approx 2.4$  and a two-peak conductance distribution at the critical point. The role of quantum coherence is discussed, and an explanation of experimental observations claiming different universality class for the quantum Hall transition is suggested. The model suggests that the critical behavior of the superconductor-insulator transition from the insulating side is in the same universality class as the quantum Hall transition.

PACS numbers: 71.30.+h, 73.43.-f, 73.43.Nq, 74.20.Mn

The integer quantum Hall (QH) effect is one of the most studied examples of a second order quantum phase transition [1]. As such it is characterized by a diverging length scale  $\xi$ , describing the typical decay of a wavefunction, or of the conductance. The physics describing the transition seems well understood, and most numerical investigations in various models yield  $\nu \simeq 2.4$  [2], where  $\nu$  describes the divergence of  $\xi$  at the critical point. Experiments, however, disagree on the critical behavior. While some indeed yield an exponent close to the theoretical prediction [3], others yield an exponent  $\nu \simeq 1.3$ , close to the classical percolation critical exponent,  $\nu_p = 4/3$  [4]. In fact, the role of percolation in the QH transition has been experimentally demonstrated [5]. Yet other experiments claim that there is no critical behavior [6].

Similar lack of clarity exists with respect to the critical exponent describing the two-dimensional superconducting-insulator transition (SIT), which can be induced either by a continuous change of film thickness, or by a magnetic field. In both cases some experiments report an exponent  $\nu$  close to 1.3 on the insulating side [7], while others yield  $\nu \simeq 2.8$  [8]. On the superconducting side only  $\nu \simeq 1.4$  has been reported. Again, similarly to the QH case, some experiments give evidence of no critical behavior [9]. The relevance of the percolation of superconducting areas to the SIT has been pointed out long time ago [10], and has been demonstrated experimentally both in granular systems [11] and in amorphous systems [12]. More recent scanning tunneling measurements [13] have directly demonstrated the separation of these systems into superconducting areas and metallic or insulating ones.

In this work we develop a generic model to describe the QH transition. This model, which is directly related to

the SIT, and to quantum percolation, clarifies the interplay of classical percolation and quantum tunneling and interference in describing the critical behavior of the QH transition. In addition to providing an estimate of the critical exponent and the fixed-point conductance distribution at the critical point, it enables us to investigate the role of tunneling and interference on the critical behavior, suggesting an explanation for the appearance of the classical critical exponent in the QH transition in some experiments [4]. Moreover, the model suggests that the SIT, on the insulating side, belongs to the same universality class as the QH transition, explaining the closeness of the numerical and experimental estimates of the critical exponents of both transitions.

The model proposed here is based on the following picture. In strong magnetic fields electrons perform small oscillations around equipotential lines. At low energies, their trajectories are trapped around potential valleys, with quantum tunneling occurring between adjacent valleys. We associate each such potential valley with a discrete lattice site, where nearest neighbors are connected by links that correspond to random tunneling between these trapped trajectories (see Fig. 1). As the Fermi energy  $\epsilon_F$  rises and crosses the saddle point energy separating two neighboring valleys, the two isolated trajectories coalesce, the electron can freely move from one valley to its neighbor and the link connecting them becomes perfect or "superconducting" (SC). The QH transition occurs when one trajectory spans the whole system, which in this lattice model corresponds to percolation of the SC links. The critical behavior, however, will be determined by the quantum mechanical processes involved in transport of an electron from one side of the system to the other, namely tunneling and interference.

For simplicity, the valleys are mapped onto sites on a square lattice. The saddle-points, which are mapped onto links in the lattice, have random energies  $\epsilon_i$ , sampled from some distribution  $G(\epsilon_i)$ . For a given Fermi energy, the transmission through the link for  $\epsilon_F < \epsilon_i$  is given by

$$T(\epsilon_F) = \exp[-\alpha(\epsilon_i - \epsilon_F)], \quad (1)$$

describing tunneling through a parabolic barrier, with  $\alpha$  a positive constant. For  $\epsilon_F > \epsilon_i$ , on the other hand, the transmission through the link is perfect (i.e.  $T(\epsilon_F) = 1$ ) and the link is considered to be SC. At low Fermi energy, very few SC links exist, and their concentration  $p(\epsilon_F)$ , given by  $p(\epsilon_F) = \int_{-\infty}^{\epsilon_F} G(\epsilon)d\epsilon$ , increases with  $\epsilon_F$ . When  $p(\epsilon_F) = p_c = \frac{61}{2}$ , the critical threshold for the square lattice, the SC links percolate through the system and the localization length diverges, signaling the QH transition. We will be interested in the critical behavior near this phase transition point [14].

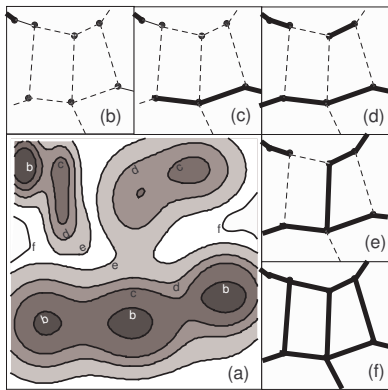


FIG. 1: Mapping of the quantum Hall system onto a discrete model. (a) Equipotential lines for five different Fermi energies. At low Fermi energies electron trajectories are confined to potential valleys. Each such valley is denoted by a point in the discrete model (b)-(f). In order to move from one such valley to another, the electron has to tunnel through a saddle point – dotted links in (b)-(f). As the Fermi energy rises above the saddle point energy these valleys are joined and electron can move without dissipation from one valley to another – solid links in (b)-(f). Figures (b)-(f) correspond to a system with Fermi energy up to the equipotential line pointed by the appropriate letter in (a). Note that in (d) the solid links percolate, meaning that at this Fermi energy an electron can traverse the whole system on an equipotential line, corresponding to the quantum Hall transition.

Two computational approaches for solving this quantum mechanical problem are presented. The first one employs a scattering matrix formalism. Each link in the lattice carries two edge states from neighboring valleys, moving in opposite directions (see Fig. 2a). The scattering matrix for each link is characterized by complex transmission and reflection amplitudes associated with

electron tunneling between adjacent valleys. The tunneling probability is determined as follows: for each link, a saddle-point energy  $\epsilon_i$  is randomly chosen from a uniform distribution  $G(\epsilon_i)$  on  $[-\frac{61}{2}, \frac{61}{2}]$  (so that the critical energy is  $\epsilon_c = 0$ , corresponding to  $p_c = \frac{61}{2}$ ). If  $\epsilon_F > \epsilon_i$  then  $T = 1$ , otherwise the transmission probability through the link is given by (1). The allowed phases of the matrix elements are chosen randomly from a uniform distribution between 0 and  $2\pi$ .

For perfect links ( $T = 1$ ), the electron follows these edge states from one valley to another, according to their chirality. It is easy to see (Fig. 2b) that when these percolate, we have two edge states propagating through the system in opposite directions, without scattering between left going and right going channels. Consequently, the percolation point corresponds to the quantum Hall transition.

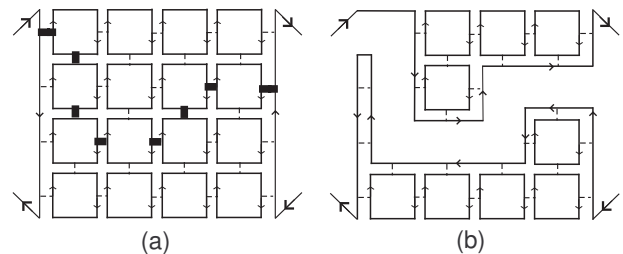


FIG. 2: The scattering matrix approach: each link carries two counter propagating edge modes (a). A non zero transmission (broken lines) allows electrons to tunnel between adjacent sites (potential valleys). When the transmission is unity (bold lines in (a)), these two valleys merge, and an edge state can freely propagate from one to another. A percolation of these perfect transmission links (b) correspond to an edge state propagating through the system without backscattering.

We evaluate the transmission  $T(L) = \exp(\langle \log T \rangle)$ , through a system of the geometry depicted in Fig. 2, of linear sizes  $L = 10, 15, \dots, 50$ , averaged over 5000 realizations, for different values of the Fermi energy near the critical point. Fig. 3 displays the raw data. In (a) we plot the dependence of the transmission on Fermi energy (in terms of probability of SC links) for different sizes. The existence of a critical point, where the curves cross and the transmission is independent of length, is evident. In (b) we show the dependence of the transmission on length for different concentrations. The inset depicts the log of the transmission as a function of length. The straight lines demonstrate that indeed,  $T(L) \propto \exp(-L/\xi(\epsilon_F))$ . All these curves coalesce (Fig. 4(a)), after scaling the system length the energy-dependent localization length  $\xi(\epsilon_F)$ .  $\xi(\epsilon_F)$  is found to diverge at the critical point with an exponent  $2.34 \pm 0.1$ , in agreement with previous numerical approaches. The inset of Fig. 4(a) displays the distribution of transmissions at the critical point. The double peak structure agrees with previous numerical calculations for the integer QHE [15].

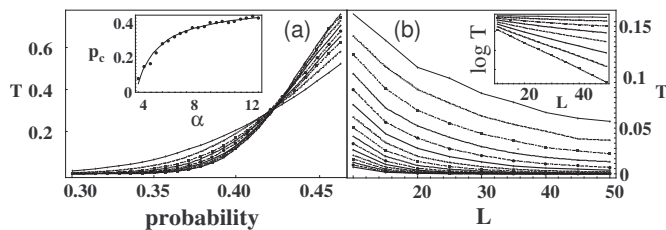


FIG. 3: Numerical results of the scattering matrix approach for  $\alpha = 12$  (see Eq. 1). (a) The transmission coefficient  $T$  as a function of Fermi energy for system lengths  $L = 10, \dots, 50$ . Inset: The dependence of the critical point on the parameter  $\alpha$ . Bold points are raw data and the solid line is the analytic curve (see text). (b) The transmission coefficient  $T$  as a function of  $L$  for different concentrations,  $p = 0.41, 0.4, \dots, 0.3$ . Inset: the same data on a semi-log plot demonstrating an  $\exp(-L/\xi(\epsilon_F))$  dependence of the transmission.

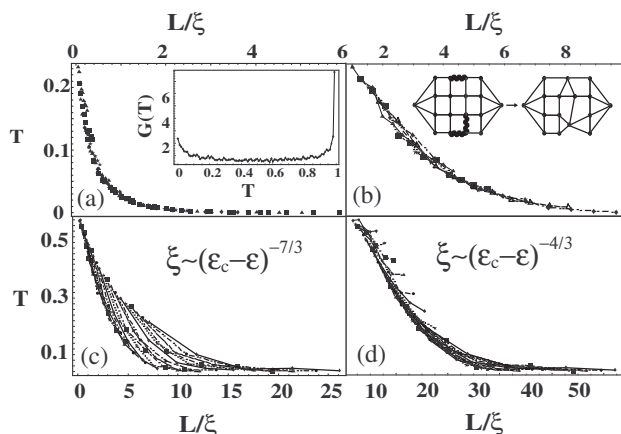


FIG. 4: (a) The raw data curves for  $T$  (Fig. 3) are collapsed onto a single curve by scaling each curve by an energy dependent localization length. This localization length diverges at the critical energy with an exponent  $2.34 \pm 0.10$ . The fixed distribution of  $T$  at the critical point is depicted in the inset. (b) Scaling of the data obtained by the tight-binding approach. For energies  $\epsilon = -0.050, -0.055, \dots, -0.1$  the data collapse yields the exponent  $\nu = 2.43 \pm 0.1$ . Inset: the tight-binding approach – sites connected by perfect links are merged and then the transmission coefficient of the modified lattice is calculated using the tight-binding hamiltonian (2). (c) Data collapse with the same exponent as in (b), including a larger range of energies  $\epsilon = -0.01, -0.02, \dots, -0.2$ . This data can be better fitted with an exponent  $\nu = 4/3$  (d).

The exponent  $\nu$  is found to be independent of the value of  $\alpha$  in (1). The critical probability, on the other hand, does depend on  $\alpha$  (inset of Fig. 3(a)). This dependence can be understood as follows: The transmission through the system at the critical point,  $T_0$ , is independent of length and of the value of  $\alpha$  and is given by an average over the fixed distribution (inset of Fig. 4(a)). As the transmission rises with Fermi energy  $\epsilon_F$ , the critical Fermi energy for a given  $\alpha$ ,  $\epsilon_c(\alpha)$ , is determined by the value of  $\epsilon_F$  at which the transmission becomes equal to  $T_0$ . Since the distribution of link transmissions is expo-

ponential, the conductance of the whole network is determined by the critical transmission, the smallest transmission value such that the links with better transmission percolate through the system [16]. This transmission is given by  $\exp[\alpha(\epsilon_c(\alpha) - \epsilon_c)]$ , with  $\epsilon_c = 0$ , the classical critical Fermi energy. Equating this transmission to  $T_0$ , one immediately finds  $\epsilon_c(\alpha) = \log(T_0)/\alpha$ , or  $p_c(\alpha) = \frac{61}{2} + \log(T_0)/\alpha$ . This function is plotted in the inset of Fig. 3(a) (solid curve), with  $T_0 = 0.4$ , and demonstrates an excellent fit to the data. The average value of  $\log(T)$  over the fixed distribution found above gives  $T_0 = 0.32$ , in rough agreement with the argument.

In order to study a model where the critical point is independent of parameters, we develop a second approach, employing a tight-binding Hamiltonian

$$\mathcal{H} = \sum_{\langle i,j \rangle} v_{ij} c_i^\dagger c_j + \text{H.c.} \quad (2)$$

Determination of the parameters  $v_{ij}$  follows the procedure described above for determining the scattering matrix parameters. We associate a random saddle-point energy  $\epsilon_{ij}$  with each link joining the lattice sites  $i$  and  $j$ . When  $\epsilon_{ij} > \epsilon_F$  the hopping matrix element  $v_{ij}$  for that link is chosen such that it will give the transmission coefficient (1). When  $\epsilon_{ij} < \epsilon_F$  the link is considered perfect, or SC. Since no value of the hopping matrix element corresponds to perfect transmission in the tight-binding approach, then when two sites are joined by such a SC link, they are merged into a single site. This guarantees that only when the SC links percolate, the conductance of the system will not decay with length, so that  $p_c$  will be independent of  $\alpha$ . The conductance is now calculated numerically, by attaching a single-channel wire to both sides of the lattice, and calculating the transmission through the system for an electron at the Fermi energy. This calculation involves two stages (see inset of Fig. 4(b)): (a) identifying clusters of sites connected by SC links as a single site, and (b) calculating  $T$  by solving the tight-binding equations in the reduced space [17]. Data is generated for lattice length  $L = 6, 10, \dots, 34$ , and averaged over 1500 realizations. Following the same scaling procedure as described above, the curves collapse onto a single curve, a procedure that yields the critical exponent  $\nu = 2.43 \pm 0.1$  (Fig. 4(b)). We also calculate the conductance distribution at the critical point and find that it shows a two-peak structure, similar to that of the S-matrix approach. Both the critical exponent and the critical point,  $p_c = \frac{61}{2}$  are independent of the parameter  $\alpha$ , for a large range of values [18]. We also check the dependence of the critical exponent  $\nu$  for different functional forms of the tunneling probability  $T(\epsilon)$  in addition to that described by (1). Using, for example, the functional form obtained by Fertig and Halperin [19], yields very similar results, with a value  $\nu = 2.49 \pm 0.1$ . A similar value is obtained when the link transmission coefficients

are taken from a uniform distribution. Thus, the model does not depend on the exact functional form of  $T(\epsilon)$ , or on its distribution. The change in the critical exponent from its classical counterpart can be traced to the fact that as the Fermi energy, or concentration of SC links, change, the transmission amplitude through the quantum insulator is modified, as the bottle-neck link changes. We also note that repeating the same calculations without random phases does not yield any reasonable scaling of the data. Thus interference effects are crucial in obtaining the correct critical behavior.

We also note that if one tries to employ the scaling analysis described above including energies that are not too close to the critical one, the collapse of the data becomes worse and in fact can be better fitted with the classical exponent  $\nu = 4/3$  (Fig. 4(c) and (d)). This is consistent with the above picture as the difference between the classical and the quantum exponents arise due to the additional dependence of the tunneling amplitude on  $\epsilon - \epsilon_c$ , a dependence that becomes less relevant away from the critical point. This observation may also explain why some experiments report a classical percolation exponent for the QH transition [4].

Since this model is practically identical to a model describing the SIT, it is not surprising that the observed critical exponents (on the insulating side) for the latter are very similar to those observed for the former. However, unlike the QH transition, the SIT is not symmetric around the critical point, which is closer to the model described here. In fact, in the superconducting phase the mechanism described above for the change in the critical exponent from its classical percolation value due to the change in the transport in the insulating phase does not have any effect. This is consistent with the experimental observations of a critical exponent close to  $\nu \approx 1.4$ , even for samples where a larger exponent was observed on the insulating side [8]. In addition, this relation between these two apparently different transitions also explains the fact that the critical resistance observed at the SIT seems to be distributed around values somewhat larger than  $h/4e^2$ , expected from duality[20]. This relation can be further investigated experimentally by studying the full resistance distribution at the SI threshold, similarly to such experiments for the QH transition[21]. The similarity of the QH transition and the SIT has already been pointed out in [22], who emphasized the non-critical behavior and the role of decoherence. In fact, the model introduced in this work allows the introduction of dephasing in a straightforward way, by attaching current-conserving, phase-breaking reservoirs to some fraction of the links [23]. The interplay between dephasing and classical-quantum crossover will be explored in a future communication [24].

We acknowledge fruitful discussions with A. Aharony and O. Entin-Wohlman. This research has been funded by the ISF.

- 
- [1] For a review see, e.g., *The Quantum Hall Effect*, edited by R. E. Prange and S. M. Girvin, Springer-Verlag, New York (1990).
  - [2] B. Huckestein, *Rev. Mod. Phys.* **67**, 357(1995).
  - [3] H. P. Wei *et al.*, *Phys. Rev. Lett.* **61**, 1294 (1988); S. Koch *et al.*, *Phys. Rev. Lett.* **67**, 883 (1991); R. J. F. Hughes *et al.*, *J.Phys.:Cond. Matt.*, **6** 4763 (1994); F. Hohls *et al.*, *Phys. Rev. Lett.* **89**, 276801 (2002).
  - [4] A. A. Shashkin *et al.*, *Phys. Rev. B* **49**, 14486 (1994); R. B. Dunford *et al.*, *Physica B*, **289** 496 (2001).
  - [5] I. V. Kukushkin *et al.*, *Phys. Rev. B* **53**, R13260 (1996); A. A. Shashkin *et al.*, *Phys. Rev. Lett.* **73**, 3141 (1994).
  - [6] D. Shahar *et al.*, *Solid. State. Comm.* **107**,19; N. Q. Balaban *et al.*, *Phys. Rev. Lett.* **81**,4967 (1998).
  - [7] D. B. Haviland, Y. Liu, and A. M. Goldman, *Phys. Rev. Lett.* **62** 2180 (1989); A. F. Hebard and M. A. Paalanen, *Phys. Rev. Lett.* **65** 927 (1990)
  - [8] Y. Liu *et al.*, *Phys. Rev. Lett.* **67** 2068 (1991); Y. Liu *et al.*, *Phys. Rev. B* **47** 5931 (1993); A. M. Goldman and Y. Liu, *Physica D*, **83** 163 (1995)
  - [9] A. Yazdani and A. Kapitulnik, *Phys. Rev. Lett.* **74**, 3037 (1995); D. Ephron *et al.*, *Phys. Rev. Lett.* **76**, 1529 (1996).
  - [10] See, e.g., G. Deutscher, Y. Imry and L. Gunther, *Phys. Rev. B* **10**, 4598 (1974).
  - [11] A. Gerber *et al.*, *Phys. Rev. Lett.* **78**, 4277 (1997).
  - [12] D. Kowal and Z. Ovadyahu, *Solid State Comm.* **90**, 783 (1994).
  - [13] A. Sharoni *et al.*, *Europhysics Lett.* **62**, 883 (2003); A. Sharoni *et al.*, *Phys. Rev. Lett.* **92**, 017003 (2004); W. Escoffier *et al.*, cond-mat/0403764.
  - [14] Our model describes the approach to criticality from one side of the critical point and, by construction, does not display the symmetry of the QHT on the two sides of the transition, in contrast to, e.g., the Chalker-Coddington model [J.T.Chalker and P.D.Coddington, *J.Phys.* **C21**, 2665 (1988)].
  - [15] D. P. Arovas, M. Janssen and B. Shapiro, *Phys. Rev. B* **56**, 4751 (1997); A. G. Galstyan and M. E. Raikh, *Phys. Rev. B* **56**, 1442 (1997); Y. Avishai, Y. Band and D. Brown, *Phys. Rev. B* **60**, 8992 (1999).
  - [16] V. Ambegaokar, B. I. Halperin and J. S. Langer, *Phys. Rev. B* **4**, 2614 (1971).
  - [17] Y. Meir, A. Aharony and A. B. Harris, *Phys. Rev. Lett.* **56**, 976 (1986).
  - [18] Near  $\alpha = 0$ , the data collapse is worse. At  $\alpha = 0$  no scaling is observed and a critical exponent cannot be determined.
  - [19] H. A. Fertig and B. I. Halperin, *Phys. Rev. B* **36**, 7969 (1995).
  - [20] See, e.g., B. G. Orr *et al.*, *Phys. Rev. Lett.* **56**, 378 (1986); S. Tayama, M. Honma and T. Takayama, *Phys. Rev. B* **43**, 8725 (1990).
  - [21] D. H. Cobden and E. Kogan, *Phys. Rev. B* **54**, R17316 (1996).
  - [22] E. Shmishoni, A. Auerbach and A. Kapitulnik, *Phys. Rev. Lett.* **80**, 3352 (1998).
  - [23] M. Buttiker, *Phys. Rev. B* **33**, 3020 (1986).
  - [24] Y. Dubi, Y. Meir and Y. Avishai, in preparation.